sustainability

MDPI

Article

Monitoring Mining Disturbance and Restoration over RBM Site in South Africa Using LandTrendr Algorithm and Landsat Data

Lubanzi Z. D. Dlamini and Sifiso Xulu *

Department of Geography and Environmental Studies, University of Zululand, KwaDlangezwa 3886, South Africa; lubanzid@gmail.com

* Correspondence: xulusi@unizulu.ac.za; Tel.: +27-035-902-6331

Received: 20 October 2019; Accepted: 21 November 2019; Published: 5 December 2019

Abstract: Considering the negative impact of mining on ecosystems in mining areas, the South African government legislated the Mineral and Petroleum Resources Development Act (No. 28 of 2002), to compel mining companies to restore the land affected by mining. Several studies have used remotely sensed data to observe the status and dynamics of surface mines. Advances in remote sensing along the cloud-based Google Earth Engine (GEE) now promise an enhanced observation strategy for improved monitoring of mine environments. Despite these advances, land rehabilitation at Richards Bay Minerals (RBM) is mainly restricted to field-based approaches which are unable to reveal seamless patterns of disturbance and restoration. Here, we illustrate the value of the trajectory-based LandTrendr algorithm in conjunction with GEE for mine rehabilitation studies. Our automated method produced disturbance and recovery patterns (1984–2018) over the RBM site. The study revealed that RBM has progressively been mining different portions of the mineral-rich coastal area after which restoration was undertaken. The duration of mining over each site ranged from 2 to 6 years. The LandTrendr outputs correspond with independent reference datasets that were classified with an overall accuracy of 99%; it captures mine-induced disturbance efficiently and offers a practical tool for mine restoration management.

Keywords: restoration; mining; Landsat; Google Earth Engine; coastal dune forest; Landtrendr; Richards Bay Minerals; KwaZulu-Natal; South Africa

1. Introduction

Since the late nineteenth century, the mining sector has played a vital role in the development of South Africa as it makes a key contribution to the country's economy, infrastructure, and employment [1,2]. The industry employed nearly 500,000 of the national labour force and contributed R349 billion (8.8%) to the country's gross domestic product in 2018 [3]. A large proportion of mining operations is concentrated in underdeveloped parts of South Africa and holds much promise for addressing the unsettled rural development agenda in the country [4]. While the economic impacts of mining have been explored broadly, the environmental and social consequences continue to receive increasing attention [5]. These repercussions include, in part, destruction of floral and faunal biodiversity [6], contamination of soil and water resources [7], and pollution caused by atmospheric dust and chemical emissions [8]. The monitoring of these outcomes is a crucial goal of sustainable development that poses a challenge for mining companies and regulatory agencies [9].

In South Africa, the Mineral and Petroleum Resources Development Act (MPRDA) (No. 28 of 2002) was passed by the government to make it compulsory for mining companies to rehabilitate the land after mining operations cease. The act requires the integration of economic, environmental,

and social aspects into all stages of the mining process to ensure optimized sustainable practices [1]. This entails mine planning, mineral extraction, and the post-mine closure stages of the operations. Overall, this application is intended to achieve a self-sustainable ecosystem at the affected site [10]. For this purpose, rehabilitation constitutes a key practice in managing and evaluating the potential effects on the Earth system affected [11]. Rehabilitation helps to reduce water pollution [12] and ameliorate the aesthetic deterioration of the natural landscape [13], which can be monitored indirectly by green vegetation, an indicator of ecosystem health and vitality [14]. The periodic and systematic evaluation of vegetation at a former mine site therefore allows assessment of the progress of the restoration process [15].

The characterization of mine revegetation success has traditionally been executed using field-based plots, which are time-consuming to do and limited in spatial coverage [16]. This is particularly a challenge for larger mining companies of the kind that is the subject of this paper. Alternatively, remote sensing presents a feasible and unbiased approach to repeatedly gather vegetation information over the entire mine sites [17]. The most common remote sensing approach for mapping and evaluating the status of vegetation within mined areas involves the use of different spectral derivatives and their band combinations such as the normalized difference vegetation index (NDVI) [18]. In the past, the examination of changes in vegetation cover relied heavily on the comparison of satellite-derived spectral indices between images acquired at two different dates, known as the bi-temporal approach [19]. Hitherto, several studies have reported the use of remote sensing to evaluate vegetation restoration over mining areas with varying degrees of success. For example, Straker et al. [20] successfully assessed the reclamation process at Bullmoose mine in British Columbia using QuickBird satellite imagery. Raval et al. [18] used WorldView-2 imagery to map surface rehabilitation at the Ulan coal mine in Australia. Bao et al. [21], with the use of SPOT-5, characterized spatial patterns of the rehabilitated landscape at Kidston gold mine in Australia using object-based image analysis and achieving high accuracies. Currently, it is impractical to monitor mine restoration solely with these commercial satellites due to their high cost and limited historical record.

The freely available Landsat images have received wide application for monitoring the progress of mining rehabilitation [11,22]. For example, Sen et al. [23] analysed the temporal profile of Landsat-derived NDVI values to characterize mining disturbances in an eastern US forested region; and they successfully classified mining from forest disturbances due to settlement expansion. Lately, the emergence of cloud-based platforms such as Google Earth Engine (GEE), combined with the entire Landsat archive [24], holds much promise for addressing progress in the rehabilitation of mining areas. These advances permit users to develop analyses that use high-density image time series to describe landscape dynamics in great detail, allowing the detection and extraction of patterns through space and time [25], and in ways that surpass traditional bi-temporal approaches. Several recent studies have demonstrated the utility of GEE-based Landsat imagery to describe vegetation changes caused by surface mining [26]. Particularly in the field of ecological restoration, there has never been a more important time than now to monitor the rehabilitation of mining areas.

A multitude of Landsat-based time series change-detection algorithms has been developed and summarized by Zhu et al. [27]. Of these, the Landsat-based detection of trends in disturbance and recovery (LandTrendr), developed by Kennedy et al. [28], has been used widely in various applications [29] and most recently in the mine restoration domain [30].

Abundant mineral resources are found in forest areas worldwide [30]; and mining has been a major forest-replacing disturbance in such areas [31,32]. This is particularly the case for Richards Bay Minerals (RBM), a dune mining company that has been extracting ilmenite, zircon, and rutile for titanium in an ecologically sensitive coastal area in the northeast of KwaZulu-Natal, South Africa [4] since 1976. The company operates in the Indian Ocean Belt forest area, an exceptionally biodiverse coastal forest that has been threatened by varied developmental pressures [33]. This could partly contribute to South Africa's 18.6% biodiversity decline since pre-industrial times, that Ott [4] attributed to industrial/commercial developmental pressures that seem to oppose biodiversity and conservation

efforts in the country [34]. Another concern is that mines have been less successful in restoring arable lands to their pre-mining productive state, particularly large open-cast mines [35]. It is therefore imperative to restore the RBM mining site as closely as possible to the original ecological conditions.

The study reported here has taken advantage of the freely available high-density Landsat data (1984–2018) and LandTrendr algorithm to explore patterns of mine-induced disturbance and subsequent land restoration over the RBM site. While previous studies have examined the progress of rehabilitation at RBM, ours is the first to provide a comprehensive trajectory-based analysis of mining disturbance and recovery over an extended period. Overall, our study demonstrates the value of an automated LandTrendr method implemented in conjunction with an affordable GEE cloud-based platform. In the following sections, we describe how LandTrendr was used within the GEE environment; we explain an analysis of LandTrendr results, and we present the validation of results followed by concluding remarks and outlooks.

2. Materials and Methods

2.1. Study Area

The study was conducted at Richards Bay Minerals, a mining area of approximately 5960 ha, located 13 km northeast of the town of Richards Bay along the mineral-rich coastal zone of KwaZulu-Natal, South Africa (Figure 1). RBM is a subsidiary of Rio Tinto, a large mining corporation with a global reach. Mining there involves the establishment of an open-cast mine in the dunes adjacent to the Indian Ocean after clearing of vegetation and flattening of the topography to create a dredge pool that gradually moves along the dune cordon. Rehabilitation is initiated when mineral extraction ceases [36]. The first operation started in 1976 with a 17-km-long and 2-km-wide coastal strip; the mining rights were further extended in 1987 for operation in the northern and southern sections [37]. The company is committed to restoring one-third of the extracted area to indigenous coastal dune forest and the remainder to commercial forest plantations [34]. So far, the RBM rehabilitation programme has received worldwide recognition as a success [37]; the results of the research reported here reveal the reality of this claim.

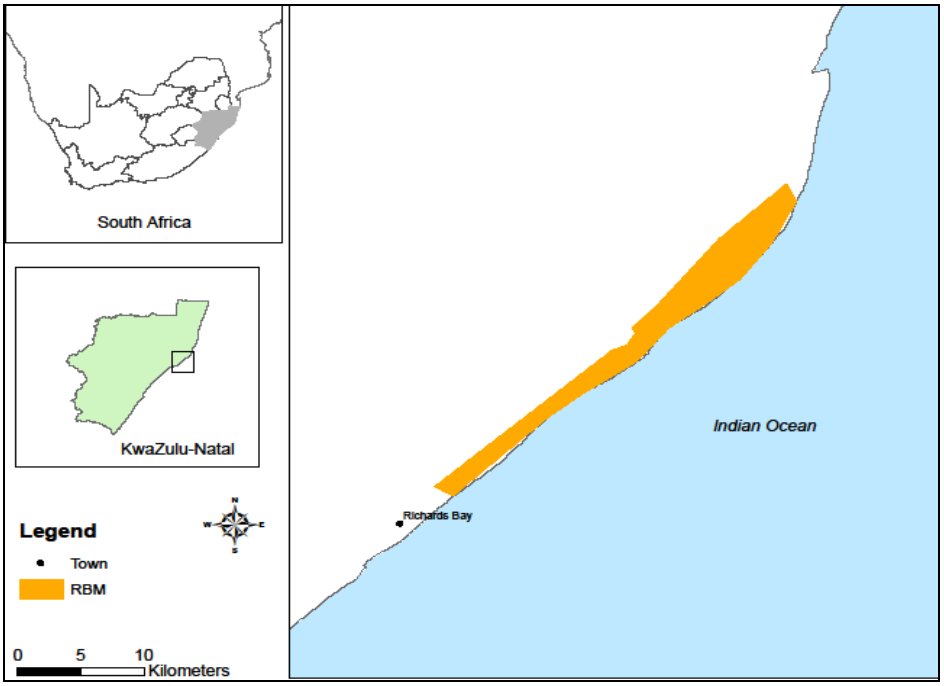

Figure 1. Location of Richards Bay Minerals, northeast of Richards Bay, along the northeast coast of KwaZulu-Natal, South Africa.

This area experiences a humid subtropical climate with rainfall peaks in February; summer temperatures are considered hot and winters warm [38]. The mean annual rainfall is 1228 mm, the mean temperatures are 29 °C in summer and 23 °C in winter. This climate is suited to vegetation regrowth and regeneration of disturbed areas [39,40]. The coastal vegetation wherein RBM's coastal dunes are situated within the Indian Ocean Coastal Belt biome is a coastal dune forest, which is an ecoregion of the Maputoland Centre of Endemism that forms part of the Maputoland–Pondoland–Albany hotspot of biological diversity [34]. Mining activities threaten an estimated 20.3% of this coastal dune forest's endemic vegetation [34,41]. RBM produces about 2.0 million tonnes of heavy minerals annually and approximately 95% of the products are exported abroad [37].

2.2. Satellite Data

We used the Landsat TM/ETM+/OLI Top of the Atmosphere Tier 1 dataset from the GEE platform as the primary source for LandTrendr, an algorithm package that extracts time series imagery information acquired by Landsat sensors; each pixel's time series is processed to simplify its temporal trajectory [28] over the period 1984 to 2018. The Landsat images are acclaimed for providing valuable information for the assessment of mine restoration processes [11,22], and their attributes—long history, fine spatial resolution, availability at no charge—make them an ideal choice for inspecting mining disturbance and rehabilitation patterns over a mining area such as RBM. The images covering path 161, row 80 were clipped using the RBM mining-permit boundary to ensure that the analysis was completely within the mining area. The images were extracted and processed using the JavaScript code editor in the GEE platform (Mountain View, CA, USA), which enables parallel computing and extensive data processing. A total of 241 Landsat images with 30-m resolution were available for analysis between 1984 and 2018. The images selected have the lowest cloud cover, to enable efficient detection of disturbance and recovery patterns. To select sites of mined plots we used Google Earth, a software that combines satellite imagery and various datasets to compile interactive, seamless true-colour satellite images of the earth [42].

2.3. Implementation of LandTrendr in GEE and Its Association with Mining Disturbance and Rehabilitation

We analyzed overall vegetation disturbance and recovery at RBM using the LandTrendr algorithm in the GEE environment. We also used the JavaScript code editor for LandTrendr as developed by Kennedy et al. [43]. Similar to numerous Landsat disturbance mapping algorithms, LandTrendr specifies a workflow designed to run using a single spectral index, while integrating many logical decision steps and statistical tests to detect disturbance [44]. The algorithm generates cloud-free mosaics from highly dense images and extracts land surface disturbance trajectories on a pixel-by-pixel basis [45]. The successful transposition of LandTrendr into the GEE platform by Kennedy et al. [43] led to its expanded application, and offers practical advantages over earlier interactive data language (IDL)-based versions [43].

To capture the mining-induced vegetation disturbance and restoration progress, the normalized difference vegetation index, calculated as the difference between near-infrared and red band reflectance normalized over their sum [46], was used. This is the most suitable index for mining-disturbance identification compared with other indexes such as the tasselled cap greenness/brightness index (TC G/B), normalized burning ratio (NBR), and normalized difference moisture index (NDMI), as reported by Li et al. [8]. The NDVI is calculated as Equation (1):

$$\mathrm{NDVI} = \frac{\mathrm{NIR} - \mathrm{Red}}{\mathrm{NIR} + \mathrm{Red}} \quad (1)$$

To identify disturbance events, LandTrendr estimates a set of vertices that connect distinct segments in NDVI time series at each pixel (Figure 2). The NDVI ranges between 1 and –1, where 1 represents a high density of green vegetation, and 0 or negative values indicate no vegetation at all. The LandTrendr outcome as illustrated in Section 3.1 reveals patterns for different stages of

mining. In this figure, t_1 represents undisturbed forested area where NDVI values are generally high. Mining entails a complete removal of forests, so that when mining starts there is a sudden drop in the NDVI curve (t_2). A period of active mining is characterized by low NDVI values (≤0.1), and this also reflects the duration of mining (t_3). When rehabilitation is implemented after mining, the NDVI curve gradually increases (t_4). After recovery of the vegetation, the NDVI trajectory can be altered by factors such as shifts in climate and clear-cut harvesting (t_5).

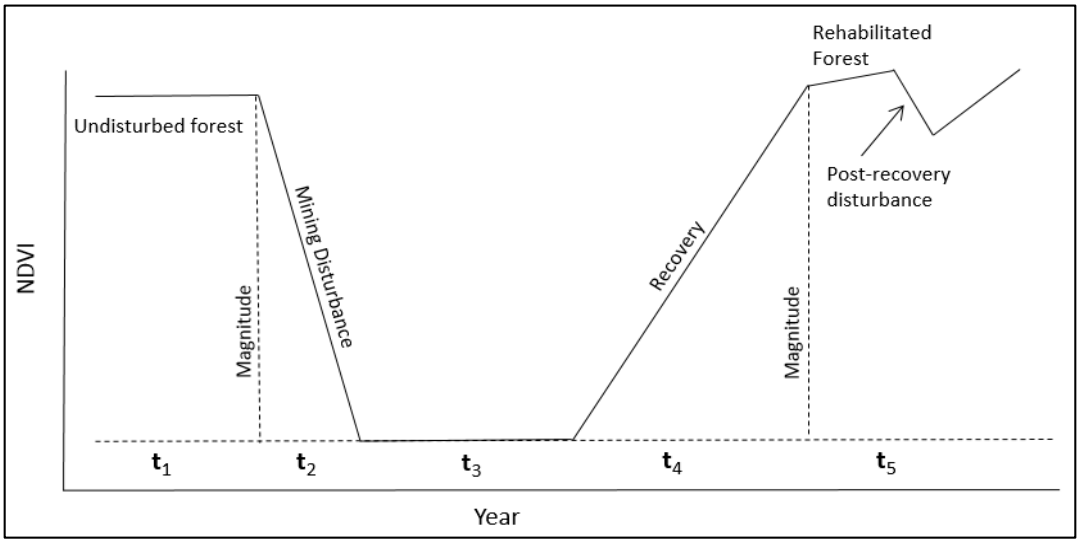

Figure 2. LandTrendr algorithm showing normalized difference vegetation index (NDVI) patterns predating, during, and postdating mining disturbances.

2.4. Validation

All maps derived from remote sensing analyses should be evaluated with completely independent datasets [30]. When no independent validation data are available, the most reliable source for assessment is the images themselves [47]. In our case, we used Google Earth, as endorsed by Yu and Gong [48], as an important tool for land cover interpretation. We applied the historical imagery function to identify mined "bare" areas on Google Earth high-resolution images with the aim of validating our results as illustrated in Figure 3. The disturbance year was identified without difficulty because of the contrast between the relatively bright patches representing active mining and forested areas displayed in images. This was repeated for different mine locations over the study period; these patches were manually labelled for each year, resulting in corresponding Keyhole Markup Language (KML)-file-formatted polygons. The ArcToolbox function "from KML to Layer" was used to create a layer, which was then exported as a shapefile. We overlaid the polygons with the LandTrendr map in the ArcMap environment and visually interpreted each polygon (see Section 3.4). It was, however, difficult to determine trajectory types for the selected sites through visual analysis. Following Yang et al. [30], we determined the trajectory analysis by inspecting the Landsat images accompanied by the NDVI temporal pattern for the selected mine sites. By viewing the images systematically, we established whether the selected sites were restored after mining operations. This was useful in discriminating mine-induced disturbances from other causes.

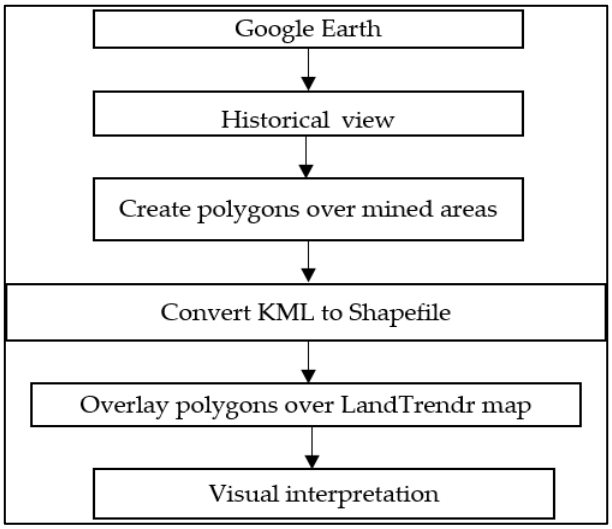

Figure 3. The process to generate the ground-truth dataset. KML: Keyhole Markup Language.

We also performed the random forests (RF; Breiman [49]) on the GEE using the "Classifier.randomforest" function available in the GEE library to assess the classification accuracy of mining and forest classes within the RBM mine. RF is the most popular ensemble learning method for classification that has increasingly gained wide application because of its high performance [50]. It partitions the data into multiple decision trees and uses a majority vote to predict the class and also requires less training time [49]. RF can be used for land cover mapping and it often gives better land cover classification accuracies [51], and hence is used as an application in this study. We generated 100 samples for each class. Thereafter, we produced a confusion matrix to estimate the overall accuracy (OA), producer accuracy (PA), and user accuracy (UA) for each category. The OA was computed by dividing the sum of correctly classified pixels by the total number of sampled pixels. The UA is computed by dividing the number of correctly classified pixels in each category by the total number of pixels that were classified in that category. The PA is calculated by dividing the number of correctly classified pixels in each category by the number of reference pixels "known" to be of that category [52,53].

$$PA = \frac{A}{A+B} \times 100 \quad (2)$$

where A is the number of pixels that were correctly classified and B is the number of pixels that were incorrectly classified.

$$UA = \frac{C}{C+D} \times 100 \quad (3)$$

where C is the number of pixels that were incorrectly classified and D is also a number of pixels that were classified correctly. The overall classification (OA) accuracies were determined by the following equation:

$$OA = \frac{A+D}{A+B+C+D} \times 100 \quad (4)$$

3. Results and Discussion

A series of 241 Landsat images were analysed to reconstruct the historical patterns of mining-induced disturbance and recovery over the RBM site between 1984 and 2018. Here, we first report the overall vegetation variations within the mining area; the NDVI patterns for each sampled site are then described. Thereafter, spatial analysis of each interim period is given, and later an accuracy assessment is performed.

3.1. Overall Spatiotemporal Patterns of Vegetation at RBM Mine 1984–2018

The LandTrendr-derived visualization of mining disturbance, as illustrated in Figure 4, shows that RBM had a definite and fairly clear configuration over the 34-year period between 1984 and 2018. From this figure, it is obvious that the company had been mining different portions of the area progressively, after which restoration was initiated. Since the mining began in 1976, prior to the base period of this study, minerals from the northeast coastal section had already been extracted in 1984. It occurred in disconnected patches of varying extents [4,54], some of which were too small to maintain ecological integrity [55]. Within the study period, mineral extraction started in the central section of the mine in 1984, adjacent to the Nhlabane Lake (Figure 2). After a further mining permit was granted in 1987 for operating the northern and southern sectors [37], the mining focus shifted southward. The mine progressed in the 2000s, where it dominated the central parts. The mine is currently more active in the north-eastern interior. In keeping with the MPRDA requirements, the results show satisfactory progress in terms of mine rehabilitation. At present, the reformed sites comprise uneven-aged commercial planted forests as well as indigenous stands, ranging in age from 5 to 38 years.

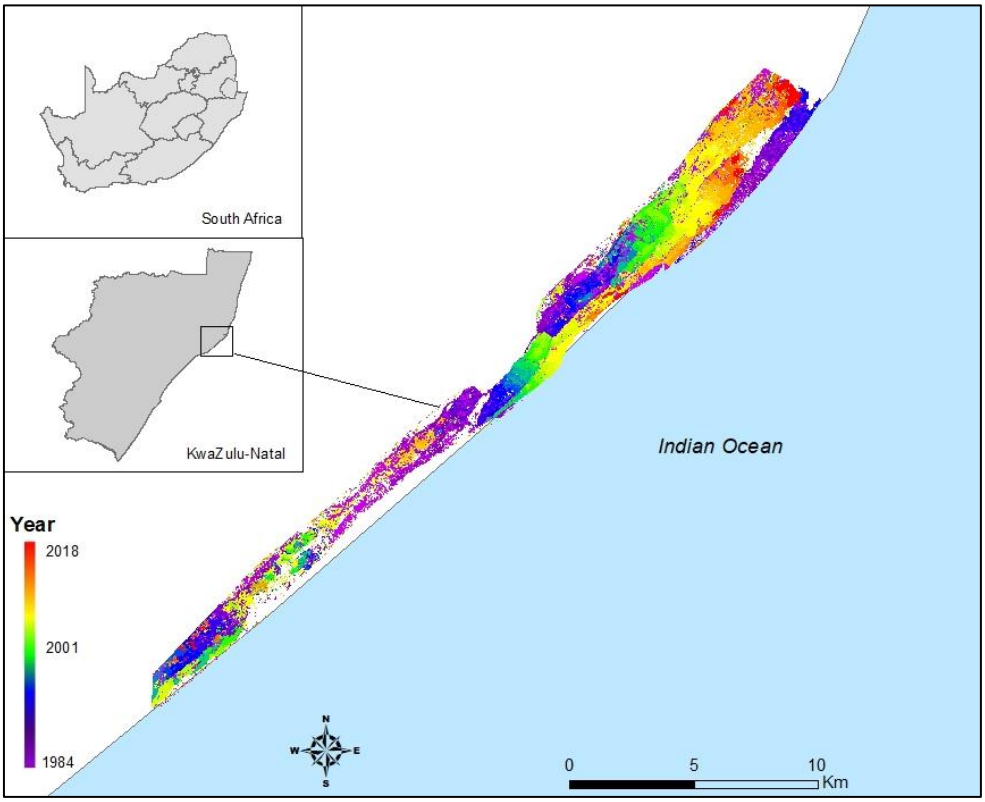

Figure 4. Landtrendr map illustrating the spatiotemporal patterns of mining disturbance at Richards Bay Minerals (RBM) from 1984 to 2018. The colour scheme represents a time sequence where the colour purple represents disturbance detected in 1984, green represents 2001, and red represents 2018.

3.2. Annual Progression of Mining Operations over RBM between 1984–2018

Figure 5 illustrates a series of NDVI maps of the RBM mining area at five-year intervals from 1984 to 2018. The results correspond well with the previous analysis of Figure 4 which indicates that the colour scheme represents a time sequence in that mining activity, as indicated by orange/yellow patches, progressed gradually from the southwest sections of the mining concession along the dune cordon towards the northeast where mining is currently active. Noteworthy is the shift of lower NDVI values (corresponding to mining) to higher values after the passage of time. Given the nature of coastal sand dunes there, the progressive greening of previously mined sites represents restoration.

These results are consistent with previous studies such as Lubke et al. [40]. Later years are dominated by higher NDVI values in the southern and central parts of the RBM mining area, all of which imply relatively successful rehabilitation as reported in [56]. This is a critical indicator of environmental sustainability performance [30]. The success of this rehabilitation project is a result of stakeholder involvement and levels of commitment from all [57].

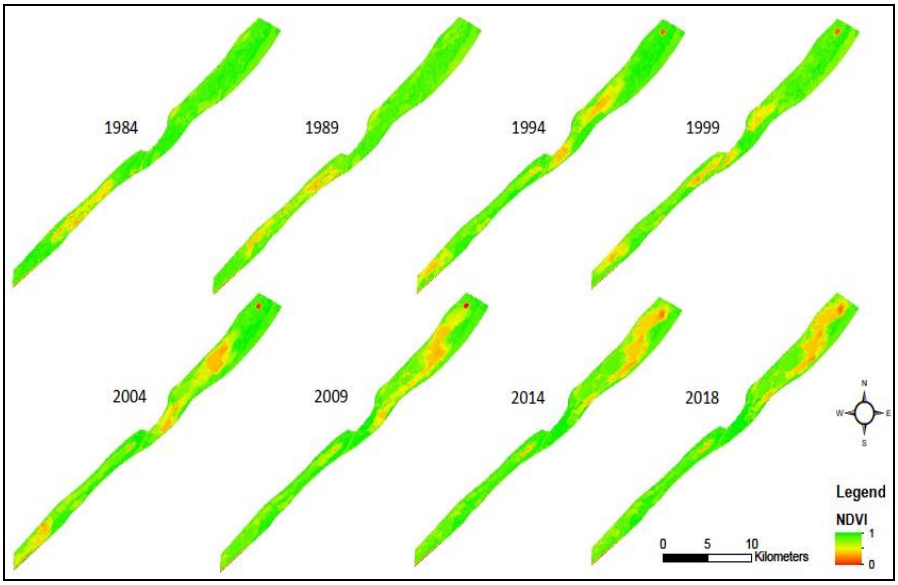

Figure 5. The spatiotemporal variability of normalized difference vegetation index (NDVI) over the Richards Bay Minerals mining area at five-year intervals for the period from 1984 to 2018. The scale represents the range of NDVI values from 0 to 1. The image for 1984, for example, shows active mining (orange) in the south-central part; 2018 indicates the result of a north-easterly progression of active mining (orange/red) and formerly mined areas now revegetated (green).

At this point, it is important to consider the temporal profiles of previous, and currently active, mining sites to understand the patterns of disturbance and recovery over the period of the study. It should be remembered that we sampled six sites that represent different time periods, the analysis of which is presented in the next section.

3.3. Temporal Profile of NDVI at Different Sites over the RBM Mine

For the first time, the temporal patterns of mining and rehabilitation over the RBM site have been analyzed in high temporal detail. Contrary to previous work, here we were able to profile the pre-dating, active, and post-dating occurrence of mining and restoration between 1984 and 2018, as shown in Figure 6. From this figure, it is clear that site 1 was altered in the early 1980s when mineral sand began to be extracted by RBM; this operation ceased in 1987. The rehabilitation began immediately after the mine closed as evidenced by the increase of NDVI from 0.05 in 1987 to 0.7 in 1990 (Figure 6). Despite signs of mining activity over RBM, there were also other noticeable disturbances. For example, the restored forest was cut in 2000, causing the NDVI to decline to 0.1. This activity did not fully obliterate the topsoil, allowing this relatively less-disturbed area to achieve a swift recovery of its vegetation cover from 2003 to 2005 and in 2010 it peaked at 0.65. A partial drop in the NDVI curve, which receded after 2016, is also notable in Figure 5, and is attributable to the recent intense drought of 2015. This observation is corroborated by Xulu et al. [58], who, using the Palmer Drought Severity Index and vegetation indices, showed that the 2015 drought strongly affected plantation forest in the same area. In this regard, it is clearly desirable for RBM's mine restoration management to consider drought-resistant trees, because more extreme drought conditions are anticipated in this region [58,59]. Mining at site 2 began in 1985 for a short stint until 1987 when the NDVI showed signs of recovery.

The partial drop of the NDVI from 1992 to 1997 is unknown. However, an obvious recovery can be seen from 1997 until the early 2000s with a slight disturbance in 2015, which is associated with drier drought conditions.

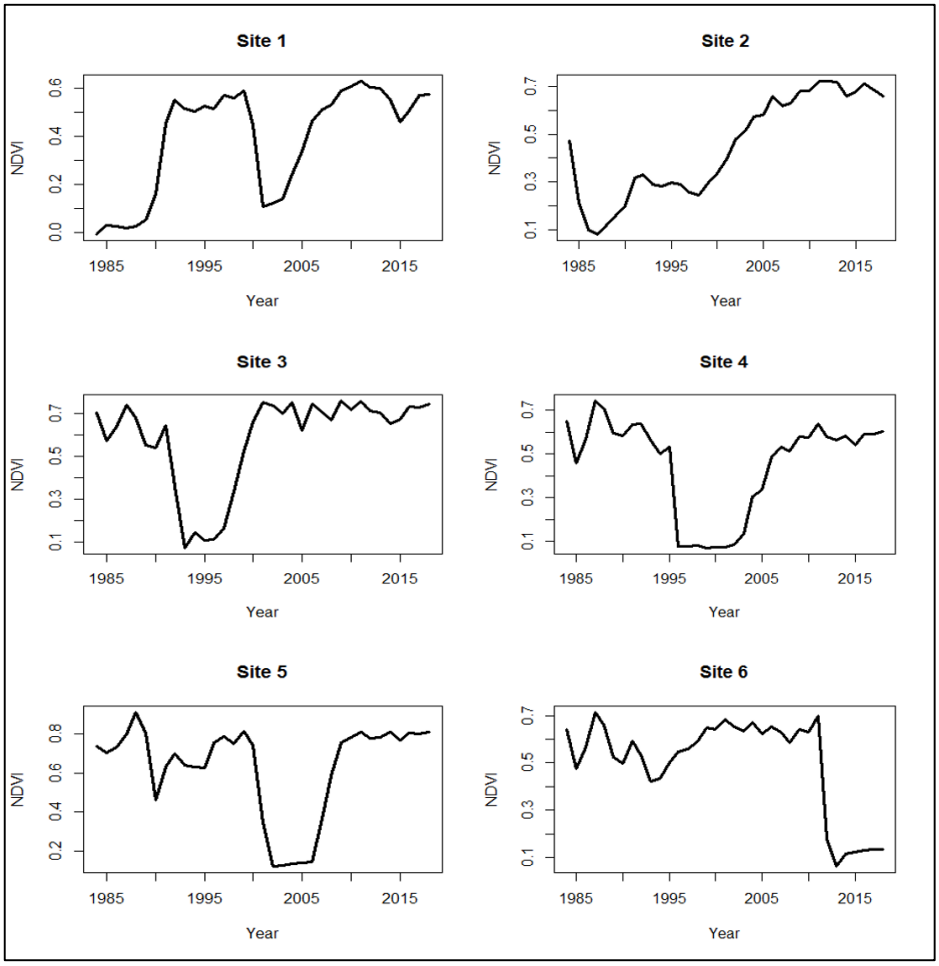

Figure 6. Temporal NDVI trajectory for sites 1–6 for the period 1984 to 2018. Higher NDVI values represent mature forest and lower values reflect mining.

Mining operations began at site 3 (Figure 6) in 1994 as evidenced by a drop in the NDVI signal; other, low-magnitude, short-lived disturbances are apparent in earlier years. These could stem from natural and anthropogenic factors but not from mining. In 1994 the NDVI value decreased from 0.63 to 0.05 and recovery was observable in 1997 (when the NDVI signal gradually rose). In the year 2000 the NDVI value increased to 0.75—a sign of restoration. As for the other locations, site 3 was responsive to the 2015 drought and vegetation recovery was noted thereafter. Sites 4 and 5 both displayed a similar trajectory to that of site 3 prior to the start of mining. Mining activity at site 4 began in 1996, when NDVI levels dropped sharply from 0.53 to 0.05. Mining was subsequently followed by recovery in 2002. The NDVI trajectory of site 5 shows the start of mining in 1998 and restoration initiated in 2006. Later in 2012, RBM began extracting mineral sands in the northern part of the concession area (site 6). This mining continues today and restoration is expected when it ceases.

Altogether, the LandTrendr algorithm appears to be an effective means to extract information on the historical disturbance and recovery dynamics of surface mining sites. With readily available GEE-cloud computing technology with global coverage, tracking mine rehabilitation is now possible even in resource-limited countries. Apart from mining-induced disturbances, LandTrendr is able to record partial disturbances associated with drought stress and anthropogenic factors. However, validation is required to ascertain the reasons for any decline in NDVI, since the spectral signal may

be affected by various factors. In our case, the decline in NDVI in 2015 at some sites was consistent with the onset of drought, as reported by Xulu et al. [60] for plantation forests in the same area, and vegetation in the adjacent Hluhluwe–Imfolozi Park [61]. Mining can be distinguished from other disturbances because vegetation was completely removed as a result and this reduced the NDVI signal to 0.1 whereas other disturbances caused only a partial decline in the NDVI value [62].

3.4. Validation

Insights regarding the relative importance of LandTrendr have been demonstrated in Sections 3.1–3.3. To examine this issue further, we validated our results by comparing LandTrendr outputs against reference mining sites as identified in the Google Earth environment (Figures 7 and 8). If the map output corresponds closely with the reference "Google Earth high-resolution imagery" data, it is considered to be accurate [63]. Our results show that the year of detection indicated by Landtrendr is comparable to the time of disturbance identified using Google Earth imagery. However, small discrepancies were noted because changes can occur in one area at different times. It should be noted that these inconsistencies were not ubiquitous but arose in certain years, particularly at the polygons corresponding to 1984 and 1991, where areas mined in those periods are expected to have a purple colour as representative of the year of destruction reported by LandTrendr, yet the 1984 polygon displays a different colour range. This detected disturbance is a result of the deforestation that occurred in that period. In the 1991 polygon the orange patches are a result of mining. According to Google Earth imagery, there was disturbance in the area and mining took place in the early 1990s although not all disturbed areas were mined. After that period of mining the area was revegetated and again in the 2000s portions that were not mined were again disturbed by mining. For all the other years the colour codes were found to correspond very with closely with the polygons; we can therefore conclude that the LandTrendr output is accurate.

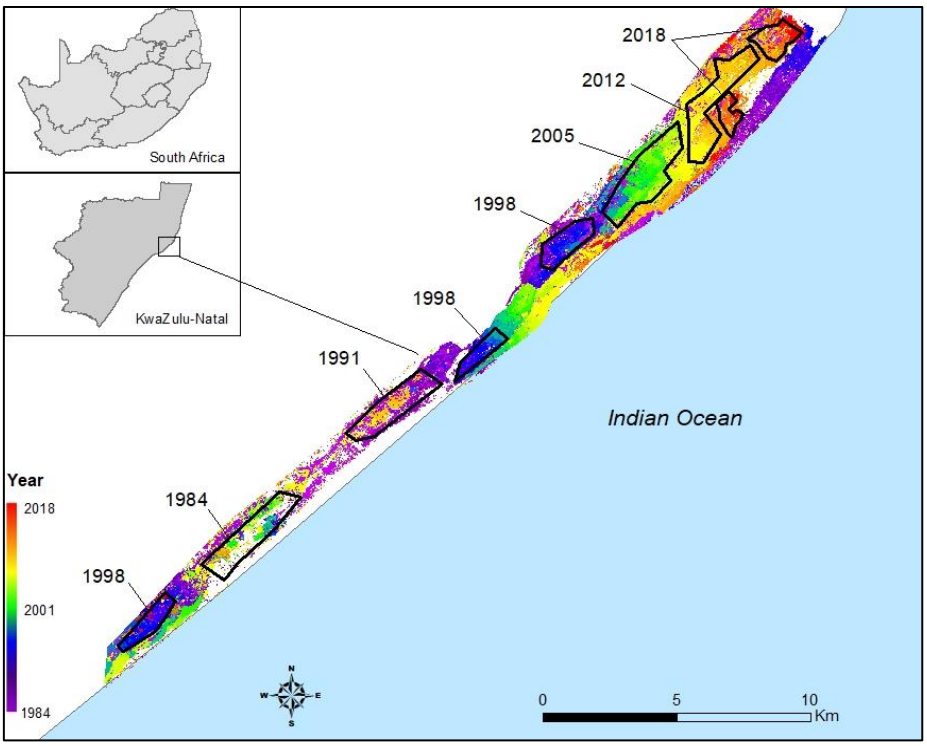

Figure 7. Validation of LandTrendr colour-coded year of detection map, overlain by Google Earth-derived polygons seven-year intervals: 1984, 1991, 1998, 2005, 2012, and 2018. Polygon-years correspond to their respective year of detection. The 1984 polygon corresponds with the purple coloured pattern and 2012 polygon corresponds with the red colour pattern.

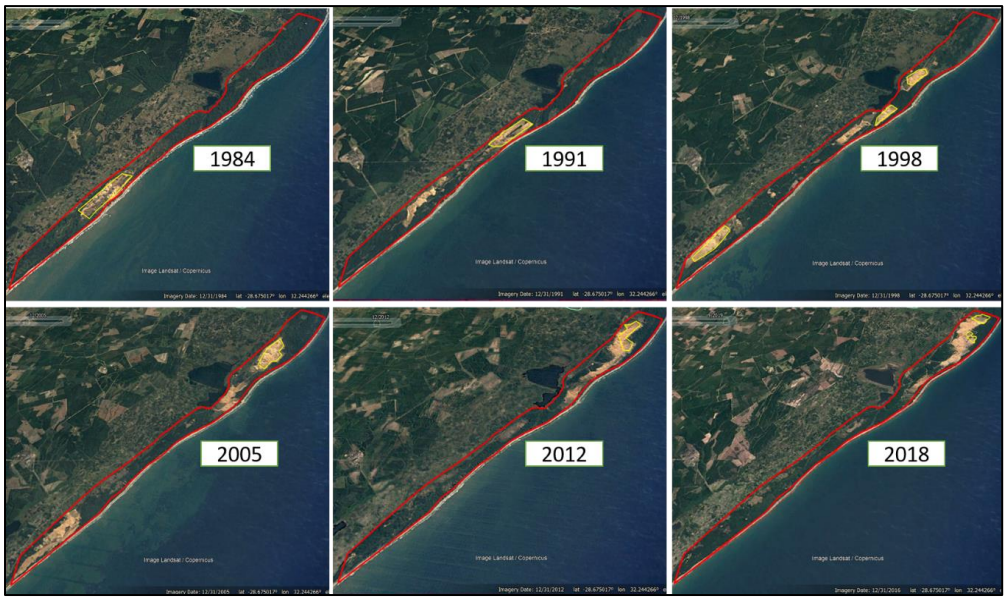

Figure 8. Google Earth high-resolution imagery showing active mining areas for different years. Mining areas are demarcated by yellow polygons and have been progressing in a northerly direction along the coast.

The RF algorithm classified mining and forest categories within RBM mining-permit area with an overall accuracy of 99%, and the classification output for 2018 is displayed in Figure 9. The producer's and user's accuracy for mining category was 100% and 99%, respectively. The forest category also achieved high corresponding accuracies of 99% and 100%. These high classification accuracies are not surprising, given the strong contrast between mining and forest spectral reflectance. These results are also consistent with Vasuki et al. [64] who applied RF to classify mining-induced land cover changes in the Darling Range mine, Australia and achieved an overall accuracy greater than 95%. Yang et al. [30] also achieved 95% accuracy in their efforts to detect disturbances associated with surface mining in Australia by means of LandTrendr and Landsat data.

Figure 9. The random forests (RF) 2018 land cover classification over RBM mine site.

Overall, the Landtrendr ensures reproducible gap-free results that characterize mining-induced disturbance and restoration patterns. The Landsat data, which are the basis of this technique, have become the preferred source of information for mine reclamation studies [10], which are expected to increase in importance given the growing application and prominence of GEE. The method is also capable of detecting non-mining disturbances such as drought and clear-cut harvesting, although field verification is required for confirmation of outputs. These results are important for countries such as South Africa that have a long troubled history of mine closure [65].

3.5. Research Limitations

One of the main limitations of using LandTrendr to monitor mining areas is that the algorithm is solely applicable to surface mining environments where land and vegetation conditions change, whereas underground mining may not greatly affect surface vegetation [30,66]. LandTrendr is most effectively exploited, therefore, when it is used to monitor surface mining and where rehabilitation has been attempted, so that progress in restoration can be tracked over time. Moreover, the outcome can be influenced by non-mining disturbances such as clear-cutting and drought, which require independent verification. Lastly, the method can only be applied for the period from 1984 onwards, depending on the availability of usable Landsat images in the region of interest.

4. Conclusions and Outlook

We have demonstrated the use of LandTrendr for characterizing patterns predating, coinciding with, and postdating heavy mineral sand extraction (1984–2018) over the RBM mining concession area along the northeast coast of South Africa. We revealed the company's spatially continuous mining operations, after which ground surface restoration was initiated when mining came to an end. The LandTrendr trajectory analysis clearly identified patterns of mine disturbance, the duration of active mining, and rehabilitation progress over the study period. The algorithm also detected non-mining disturbances such as drought-stress and clear-cut harvesting at the restored sites and affirmed the relative success of RBM's restoration programme. This practical tool can complement ecological field studies of disturbed and restored landscapes, and the use of higher resolution images such as freely available Sentinel-2 can greatly improve this method.

In the future, studying the spectral behavior of both the restored native and commercial forests in the areas of interest by this means should enable improved understanding of their development, including their reaction to non-mining post-disturbance events such as droughts. This could assist restoration management in selecting plant species that are resistant to these stressors. It would also be desirable to detect mineral properties before and after mining operations to understand conditions under which restoration is best carried out. Lastly, the mining authorities, scientists, and the government need inexpensive and easily accessible information for characterizing disturbance and recovery patterns of mining under their purview. The GEE-based LandTrendr algorithm presents opportunities for improved and quick retrieval of datasets to understand mining-induced disturbances and restoration patterns over varying scales, so that mine restoration strategies can be improved. Our method is relatively versatile as it can be applied directly to other land surface change scenarios and should produce equally reliable results. Moreover, it can easily be applied to other regions, including those in resource-poor countries.

Author Contributions: L.Z.D.D. and S.X. contributed equally to the conceptualization, validation, and supervision of this project, and to the writing of the paper.

Funding: This research was partly funded by the National Research Foundation (NRF) of South Africa and the APC was funded by the University of Zululand.

Acknowledgments: The authors would like to thank all personnel involved in the development of the Google Earth Engine-based LandTrendr code. We are also thankful for the comments and suggestions of the anonymous reviewers.

Conflicts of Interest: The authors declare no conflicts of interest.

References

1. Swart, E. The South African legislative framework for mine closure. *J. S. Afr. Inst. Min. Metall.* **2003**, *103*, 489–492.
2. Tanner, P. *Guidelines for the Rehabilitation of Mined Land*; Chamber of Mines South Africa Press: Johannesburg, South Africa, 2007.
3. Casey, J.P. The Future of Mining in South Africa. 2019. Available online: https://www.mining--technology.com/features/the--future--of--mining--in--south--africa/ (accessed on 30 August 2019).
4. Ott, T. Finding the interface between mining, people, and biodiversity: A case study at Richards Bay Minerals. *J. S. Afr. Inst. Min. Metall.* **2017**, *117*, 1–5. [CrossRef]
5. Sincovich, A.; Gregory, T.; Wilson, A.; Brinkman, S. The social impacts of mining on local communities in Australia. *Rural Soc.* **2018**, *27*, 18–34. [CrossRef]
6. Zhang, A.; Moffat, K. A balancing act: The role of benefits, impacts and confidence in governance in predicting acceptance of mining in Australia. *Resour. Policy* **2015**, *44*, 25–34. [CrossRef]
7. Pourret, O.; Lange, B.; Bonhoure, J.; Colinet, G.; Decrée, S.; Mahy, G.; Séleck, M.; Shutcha, M.; Faucon, M.P. Assessment of soil metal distribution and environmental impact of mining in Katanga (Democratic Republic of Congo). *Appl. Geochem.* **2016**, *64*, 43–55. [CrossRef]
8. Li, Z.; Ma, Z.; van der Kuijp, T.J.; Yuan, Z.; Huang, L. A review of soil heavy metal pollution from mines in China: Pollution and health risk assessment. *Sci. Total Environ.* **2014**, *468*, 843–853. [CrossRef]
9. Sonter, L.J.; Moran, C.J.; Barrett, D.J.; Soares–Filho, B.S. Processes of land use change in mining regions. *J. Clean. Prod.* **2014**, *84*, 494–501. [CrossRef]
10. Elmqvist, T.; Folke, C.; Nyström, M.; Peterson, G.; Bengtsson, J.; Walker, B.; Norberg, J. Response diversity, ecosystem change, and resilience. *Front. Ecol. Environ.* **2003**, *1*, 488–494. [CrossRef]
11. Petropoulos, G.P.; Partsinevelos, P.; Mitraka, Z. Change detection of surface mining activity and reclamation based on a machine learning approach of multi–temporal Landsat TM imagery. *Geocarto Int.* **2013**, *28*, 323–342. [CrossRef]
12. Latifovic, R.; Fytas, K.; Chen, J.; Paraszczak, J. Assessing land cover change resulting from large surface mining development. *Int. J. Appl. Earth Obs. Geoinform.* **2005**, *7*, 29–48. [CrossRef]
13. Gesch, D.B. Analysis of multi-temporal geospatial data sets to assess the landscape effects of surface mining. In Proceedings of the National Meeting of the American Society of Mining and Reclamation, Lexington, KY, USA, 19–23 June 2005; pp. 415–432.
14. Du, H.; Cui, R.; Zhou, G.; Shi, Y.; Xu, X.; Fan, W.; Lü, Y. The responses of Moso bamboo (Phyllostachys heterocycla var. pubescens) forest aboveground biomass to Landsat TM spectral reflectance and NDVI. *Acta Ecol. Sin.* **2010**, *30*, 257–263. [CrossRef]
15. De Simoni, B.S.; Leite, M.G.P. Assessment of rehabilitation projects results of a gold mine area using landscape function analysis. *Appl. Geogr.* **2019**, *108*, 22–29. [CrossRef]
16. Kariyawasam, N.; Raval, S.; Shamsoddini, A. Incorporating Remote Sensing as a Tool to Assist rehabilitation monitoring in a dolomite mining operation in South Australia. In Proceedings of the XXV FIG INTERNATIONAL CONGRESS, Kuala Lumpur, Malaysia, 16–21 June 2014; International Federation of Surveyors (FIG) Press: Kuala Lumpur, Malaysia, 2014; pp. 1–13. Available online: http://www.fig.net/pub/fig2014/papers/ts08b/TS08B_kariyawasam_raval_et_al_6966.pdf (accessed on 19 September 2019).
17. Whiteside, T.G.; Bartolo, R.E. A robust object-based woody cover extraction technique for monitoring mine site revegetation at scale in the monsoonal tropics using multispectral RPAS imagery from different sensors. *Int. J. Appl. Earth Obs. Geoinform.* **2018**, *73*, 300–312. [CrossRef]
18. Raval, S.; Merton, R.N.; Laurence, D. Satellite Based Mine Rehabilitation Monitoring Using WorldView-2 Imagery. *Min. Technol.* **2013**, *122*, 200–207. [CrossRef]
19. Coppin, P.; Jonckheere, I.; Nackaerts, K.; Muys, B.; Lambin, E. Review article digital change detection methods in ecosystem monitoring: A review. *Int. J. Remote Sens.* **2004**, *25*, 1565–1596. [CrossRef]
20. Straker, J.; Blazecka, M.; Sharman, K.; Woelk, S.; Boorman, S.; Kuschminder, J. Use of remote sensing in reclamation assessment. In Proceedings of the 28th Annual Mine Reclamation Symposium, Teck Cominco's Bullmoose Mine Site, Cranbrook, BC, Canada, 23 June 2004.

21. Bao, N.; Lechner, A.M.; Johansen, K.; Ye, B. Object-based classification of semi-arid vegetation to support mine rehabilitation and monitoring. *J. Appl. Remote Sens.* **2014**, *8*, 083564. [CrossRef]
22. Bonifazi, G.; Cutaia, L.; Massacci, P.; Roselli, I. Monitoring of abandoned quarries by remote sensing and in situ surveying. *Ecol. Model.* **2003**, *170*, 213–218. [CrossRef]
23. Sen, S.; Zipper, C.E.; Wynne, R.H.; Donovan, P.F. Identifying revegetated mines as disturbance/recovery trajectories using an interannual Landsat chronosequence. *Photogramm. Eng. Remote Sens.* **2012**, *78*, 223–235. [CrossRef]
24. Gorelick, N.; Hancher, M.; Dixon, M.; Ilyushchenko, S.; Thau, D.; Moore, R. Google Earth Engine: Planetary–scale geospatial analysis for everyone. *Remote Sens. Environ.* **2017**, *202*, 18–27. [CrossRef]
25. Kennedy, R.E.; Andréfouët, S.; Cohen, W.B.; Gómez, C.; Griffiths, P.; Hais, M.; Healey, S.P.; Helmer, E.H.; Hostert, P.; Lyons, M.B.; et al. Bringing an ecological view of change to Landsat-based remote sensing. *Front. Ecol. Environ.* **2014**, *12*, 339–346. [CrossRef]
26. Pericak, A.A.; Thomas, C.J.; Kroodsma, D.A.; Wasson, M.F.; Ross, M.R.; Clinton, N.E.; Campagna, D.J.; Franklin, Y.; Bernhardt, E.S.; Amos, J.F. Mapping the yearly extent of surface coal mining in Central Appalachia using Landsat and Google Earth Engine. *PLoS ONE* **2018**, *13*, 0197758. [CrossRef] [PubMed]
27. Zhu, Z. Change detection using Landsat time series: A review of frequencies, preprocessing, algorithms, and applications. *ISPRS J. Photogramm. Remote Sens.* **2017**, *130*, 370–384. [CrossRef]
28. Kennedy, R.E.; Yang, Z.; Cohen, W.B. Detecting trends in forest disturbance and recovery using yearly Landsat time series: 1. LandTrendr—Temporal segmentation algorithms. *Remote Sens. Environ.* **2010**, *114*, 2897–2910. [CrossRef]
29. Pflugmacher, D.; Cohen, W.B.; Kennedy, R.E.; Yang, Z. Using Landsat-derived disturbance and recovery history and Lidar to map forest biomass dynamics. *Remote Sens. Environ.* **2014**, *151*, 124–137. [CrossRef]
30. Yang, Y.; Erskine, P.D.; Lechner, A.M.; Mulligan, D.; Zhang, S.; Wang, Z. Detecting the dynamics of vegetation disturbance and recovery in surface mining area via Landsat imagery and LandTrendr algorithm. *J. Clean. Prod.* **2018**, *178*, 353–362. [CrossRef]
31. Minnemeyer, S.; Laestadius, L.; Potapov, P.; Sizer, N.; Saint-Laurent, C. *Atlas of Forest Landscape Restoration Opportunities*; World Resources Institute Press: Washington, DC, USA, 2014.
32. Macdonald, S.E.; Landhäusser, S.M.; Skousen, J.; Franklin, J.; Frouz, J.; Hall, S.; Jacobs, D.F.; Quideau, S. Forest restoration following surface mining disturbance: Challenges and solutions. *New For.* **2015**, *46*, 703–732. [CrossRef]
33. Smith, D.A.E.; Smith, Y.C.E.; Downs, C.T. Indian Ocean coastal thicket is of high conservation value for preserving taxonomic and functional diversity of forest-dependent bird communities in a landscape of restricted forest availability. *For. Ecol. Manag.* **2017**, *390*, 157–165. [CrossRef]
34. Grainger, M.J. An Evaluation of Coastal Dune Forest Restoration in Northern KwaZulu-Natal. Ph.D. Thesis, University of Pretoria, Pretoria, South Africa, 2011.
35. Limpitlaw, D.; Aken, M.; Lodewijks, H.; Viljoen, J. Post-mining rehabilitation, land use and pollution at collieries in South Africa. In Proceedings of the Colloquium: Sustainable Development in the Life of Coal Mining, South African Institute of Mining and Metallurgy, Boksburg, South Africa, 13 July 2005.
36. West, A.; Bond, W.; Midgley, J.J. Dune forest succession on old lands: Implications for post-mining restoration. Towards sustainable management based on scientific understanding of natural forests and woodlands. In Proceedings of the Natural Forests and Woodlands Symposium II, Department of Water Affairs and Forestry, Knysna, South Africa, 5–9 September 1999; pp. 35–39.
37. Williams, G.E.; Steenkamp, J.D. *Heavy Minerals Processing at Richards Bay Minerals; South African Pyrometallurgy*; Jones, R.T., Ed.; South African Institute of Mining and Metallurgy: Johannesburg, South Africa, 2006.
38. DWAF (Department of Water Affairs and Forestry). *Water Resource Protection and Assessment Policy Implementation Process. Resource Directed Measures for Protection of Water Resource: Methodology for the Determination of the Ecological Water Requirements for Estuaries*; Department of Water Affairs and Forestry: Pretoria, South Africa, 2004.
39. Moll, J.B. Studies on Dune Rehabilitation Techniques for Mined Areas at Richards Bay, Natal. Ph.D. Thesis, Rhodes University, Grahamstown, South Africa, 1992.

40. Lubke, R.A.; Avis, A.M.; Moll, J.B. Post-mining rehabilitation of coastal sand dunes in Zululand South Africa. *Landsc. Urban Plan.* **1996**, *34*, 335–345. [CrossRef]
41. Wooley, L. An Assessment of the Conservation Status of Coastal Dune Forest in the Maputaland Centre of Endemism using Landsat TM imagery. Master's Thesis, University of Pretoria, Pretoria, South Africa, 2003.
42. Choi, Y.; Nieto, A. Optimal haulage routing of off-road dump trucks in construction and mining sites using Google Earth and a modified least-cost path algorithm. *Autom. Constr.* **2011**, *20*, 982–997. [CrossRef]
43. Kennedy, R.; Yang, Z.; Gorelick, N.; Braaten, J.; Cavalcante, L.; Cohen, W.; Healey, S. Implementation of the LandTrendr algorithm on Google Earth Engine. *Remote Sens.* **2018**, *10*, 691. [CrossRef]
44. Cohen, W.B.; Yang, Z.; Healey, S.P.; Kennedy, R.E.; Gorelick, N. A LandTrendr multispectral ensemble for forest disturbance detection. *Remote Sens. Environ.* **2018**, *205*, 131–140. [CrossRef]
45. Runge, A.; Groose, G. Applying both Landsat and Sentinl-2 data to Landtrendr for detection of landscape change trends in Arctic permafrost regions. In Proceedings of the ESA Living Planet Symposium, Milan, Italy, 13–17 May 2019.
46. Tucker, C.J. Red and photographic infrared linear combinations for monitoring vegetation. *Remote Sens. Environ.* **1979**, *8*, 127–150. [CrossRef]
47. Kennedy, R.E.; Cohen, W.B.; Schroeder, T.A. Trajectory-based change detection for automated characterization of forest disturbance dynamics. *Remote Sens. Environ.* **2007**, *110*, 370–386. [CrossRef]
48. Yu, L.; Gong, P. Google Earth as a virtual globe tool for Earth science applications at the global scale: Progress and perspectives. *Int. J. Remote Sens.* **2012**, *33*, 3966–3986. [CrossRef]
49. Breiman, L. Random forests. *Mach. Learn.* **2001**, *45*, 5–32. [CrossRef]
50. Kulkarni, A.D.; Lowe, B. Random forest algorithm for land cover classification. *Pattern Recognit. Lett.* **2016**, *27*, 294–300.
51. Balzter, H.; Cole, B.; Thiel, C.; Schmullius, C. Mapping CORINE land cover from Sentinel-1A SAR and SRTM digital elevation model data using Random Forests. *Remote Sens.* **2015**, *7*, 14876–14898. [CrossRef]
52. Unger, D.R.; Hung, I.K.; Kulhavy, D.L. Accuracy assessment of land cover maps of forests within an urban and rural environment. *For. Sci.* **2013**, *60*, 591–602. [CrossRef]
53. Peerbhay, K.; Mutanga, O.; Lottering, R.; Ismail, R. Mapping Solanum mauritianum plant invasions using WorldView-2 imagery and unsupervised random forests. *Remote Sens. Environ.* **2016**, *182*, 39–48. [CrossRef]
54. Weisser, P.J.; Marques, F. Gross vegetation changes in the dune area between Richards Bay and the Mfolozi River, 1937–1974. *Bothalia* **1979**, *12*, 711–721. [CrossRef]
55. Olivier, P.I.; van Aarde, R.J.; Lombard, A.T. The use of habitat suitability models and species–area relationships to predict extinction debts in coastal forests, South Africa. *Divers. Distrib.* **2013**, *19*, 1353–1365. [CrossRef]
56. Pranato, A.K.; Gikes, B.; Mengler, F.C. The use of remotely sensed data to analyze spatial and temporal trends in patchiness within rehabilitated bauxite mines in the Darling Range. In Proceedings of the 3rd Australian New Zealand Soils Conference, University of Sydney, Sydney, Australia, 5–9 December 2004.
57. Macfarlane, A.S. Of sun, shells, sand, and sea. *J. S. Afr. Min Metall.* **2019**, *119*, 5–6.
58. Xulu, S.; Peerbhay, K.; Gebreslasie, M.; Ismail, R. Drought influence on forest plantations in Zululand, South Africa, using MODIS time series and climate data. *Forest* **2018**, *9*, 528. [CrossRef]
59. Nhamo, L. *Trends and Outlook: Agricultural Water Management in Southern Africa*; SADC Agwater Profiles; International Water Management Institute (IWMI), Southern Africa Regional Office: Pretoria, South Africa, 2015.
60. Xulu, S.; Peerbhay, K.; Gebreslasie, M.; Ismail, R. Unsupervised clustering of forest response to drought stress in Zululand region, South Africa. *Forest* **2019**, *10*, 531. [CrossRef]
61. Mbatha, N.; Xulu, S. Time series analysis of MODIS–derived NDVI for the Hluhluwe-Imfolozi Park, South Africa: Impact of recent intense drought. *Climate* **2018**, *6*, 95. [CrossRef]
62. Ahmed, N. Application of NDVI in vegetation monitoring using GIS and remote sensing in northern Ethiopian highlands. *Abyss J. Sci. Technol.* **2016**, *1*, 12–17.
63. Campbell, J.B.; Wynne, R.H. *Introduction to Remote Sensing*, 5th ed.; Guilford Press: New York, NY, USA, 2011.
64. Vasuki, Y.; Yu, L.; Holden, E.J.; Kovesi, P.; Wedge, D.; Grigg, A.H. The spatial-temporal patterns of land cover changes due to mining activities in the Darling Range, Western Australia: A Visual Analytics Approach. *Ore Geol. Rev.* **2019**, *108*, 23–32. [CrossRef]

65. Krause, R.D.; Synman, L.G. Rehabilitation and mine closure liability: An assessment of accountability of the systems to communities. In Proceedings of the 9th International Conference of Mine Closure, Sandton, Johannesburg, South Africa, 1–3 October 2014.
66. Lechner, A.M.; Baumgartl, T.; Matthew, P. The impact of underground longwall mining on prime agricultural land: A review and research agenda. *Land Degrad. Dev.* **2016**, *27*, 1650–1663. [CrossRef]